

Super-strong interactions between multivalent anions and graphene

Xing Liu(刘星) and Guosheng Shi(石国升)†
Citation: Chin. Phys. B, 2021, 30 (**4**): 046801. DOI: 10.1088/1674-1056/abd396
Journal homepage: http://cpb.iphy.ac.cn; http://iopscience.iop.org/cpb

What follows is a list of articles you may be interested in

First principles study of behavior of helium at Fe(110)-graphene interface

Yan-Mei Jing(荆艳梅) and Shao-Song Huang(黄绍松)
Chin. Phys. B, 2021, 30 (**4**): 046802. DOI: 10.1088/1674-1056/abd46d

Interfaces between MoO_x and MoX_2 (X = S, Se, and Te)

Fengming Chen(陈凤鸣), Jinxin Liu(刘金鑫), Xiaoming Zheng(郑晓明), Longhui Liu(刘龙慧), Haipeng Xie(谢海鹏), Fei Song(宋飞), Yongli Gao(高永立), and Han Huang(黄寒)
Chin. Phys. B, 2020, 29 (**11**): 116802. DOI: 10.1088/1674-1056/abb310

Covalent coupling of DNA bases with graphene nanoribbon electrodes: Negative differential resistance, rectifying, and thermoelectric performance

Peng-Peng Zhang(张鹏鹏), Shi-Hua Tan(谭仕华)†, Xiao-Fang Peng(彭小芳)‡, and Meng-Qiu Long(龙孟秋)
Chin. Phys. B, 2020, 29 (**10**): 106801. DOI: 10.1088/1674-1056/aba9bf

Triphenylene adsorption on Cu(111) and relevant graphene self-assembly

Qiao-Yue Chen(陈乔悦), Jun-Jie Song(宋俊杰), Liwei Jing(井立威), Kaikai Huang(黄凯凯), Pimo He(何丕模), Hanjie Zhang(张寒洁)
Chin. Phys. B, 2020, 29 (**2**): 026801. DOI: 10.1088/1674-1056/ab6583

Adsorption behavior of triphenylene on Ru(0001) investigated by scanning tunneling microscopy

Li-Wei Jing(井立威), Jun-Jie Song(宋俊杰), Yu-Xi Zhang(张羽溪), Qiao-Yue Chen(陈乔悦), Kai-Kai Huang(黄凯凯), Han-Jie Zhang(张寒洁), Pi-Mo He(何丕模)
Chin. Phys. B, 2019, 28 (**7**): 076801. DOI: 10.1088/1674-1056/28/7/076801

Super-strong interactions between multivalent anions and graphene*

Xing Liu(刘星)[1] and Guosheng Shi(石国升)[1,2,†]

[1] Shanghai Applied Radiation Institute, State Key Laboratory Advanced Special Steel, Shanghai University, Shanghai 200444, China
[2] Division of Interfacial Water and Key Laboratory of Interfacial Physics and Technology, Shanghai Institute of Applied Physics, Chinese Academy of Sciences, Shanghai 201800, China

(Received 19 October 2020; revised manuscript received 19 November 2020; accepted manuscript online 15 December 2020)

Based on the density functional theory (DFT) calculations, we showed that the interactions between different valence anions (PO_4^{3-}, $CH_3PO_4^{2-}$, $(CH_3)_2PO_4^-$) and graphene significantly increased as the valence of anion increased from negative monovalence to negative trivalence. The adsorption energy of $(CH_3)_2PO_4^-$ on the electron-rich graphene flake ($C_{84}H_{24}$) is −8.3 kcal/mol. The adsorption energy of $CH_3PO_4^{2-}$ on the electron-rich graphene flake ($C_{84}H_{24}$) is −48.0 kcal/mol, which is about six times that of $(CH_3)_2PO_4^-$ adsorption on electron-rich graphene flake ($C_{84}H_{24}$) and is even much larger than that of CO_3^{2-} adsorption on electron-deficient aromatic ring C_6F_6 (−28.4 kcal/mol). The adsorption energy of PO_4^{3-} on the electron-rich graphene flake ($C_{84}H_{24}$) is −159.2 kcal/mol, which is about 20 times that of $(CH_3)_2PO_4^-$ adsorption on the graphene flake ($C_{84}H_{24}$). The super-strong adsorption energy is mainly attributed to the orbital interactions between multivalent anions and graphene. This work provides new insights for understanding the interaction between multivalent anions and π–electron-rich carbon-based nanomaterials and is helpful for the design of graphene-based DNA biosensor.

Keywords: graphene, multivalent anions, anion–π interaction, density functional theory

PACS: 81.05.ue, 68.43.–h, 31.15.E **DOI:** 10.1088/1674-1056/abd396

1. Introduction

Anion–π interactions play important roles in various chemical and biological processes,[1–14] such as supramolecular self-assembly,[10] inhibition of the enzymatic activity,[7] design of selective anion receptors, and molecular recognition of anion.[6] Generally, anion–π interactions involved the interactions between anion and electron-deficient substrate, such as interaction between anions and hexafluorobenzene (C_6F_6).[1,4,15] For the simplest aromatic ring with π electron-rich structure benzene (C_6H_6), previous research[16] showed that the binding energy between F^- and C_6H_6 was 1.5 kcal/mol and the binding energy between Cl^- and C_6H_6 was 1.1 kcal/mol, which indicated the unfavorable adsorption of common halide ion (F^- and Cl^-) on the simple benzene (C_6H_6). However, researchers find unexpectedly strong anion–π interactions between halide ions and the graphene flake containing multi-aromatic rings with π electron-rich structures,[17,18] for example, the adsorption energy between F^- and the graphene flake was as large as −16.3 kcal/mol.[17,18] Nowadays, the research about anion–π interactions mainly focused on the interactions between monovalent anions (F^-, Cl^-, Br^-, CN^-, NO_3^-, *etc.*),[1,4,5,8,13,16] and electron-deficient substrate, some divalent anions have also been reported, such as the adsorption energy between CO_3^{2-} and C_6F_6 was −28.4 kcal/mol, which was larger than that between monovalent halide ions with C_6F_6.[1] Recently, combined the experiment and theoretical computations,[14] researcher reported anion–π–cation interaction between different anions and methyl amide of the π-conjugated quinone (QMA)–K^+ pair in aqueous solution and showed the anion–π interactions follow the trend phosphate ester $>HPO_4^{2-}>SO_4^{2-}>NO_3^-$. However, the anion–π interactions between multivalent anions and electron-rich graphene still remains unknown.

Recently, graphene/graphene oxide (GO)-based materials have been employed for the development of DNA biosensors and are widely used in genetics, clinical medicine, pathology, and many other fields.[19–23] These applications are related to the interaction between graphene/GO and DNA.[24–26] However, most researches focused on the interaction between nucleic acid bases and graphene,[27–30] the interaction of backbone phosphate groups are ignored. As an important component of DNA/RNA backbone, phosphate groups played important roles in biochemistry.[31] In the backbone of DNA/RNA, phosphoric group links two nucleotides and still ionized as monovalent anion. At the termini of DNA/RNA, phosphoric group is bivalent anion.[32] Thus, it is necessary to investigate the interaction between phosphate groups with different valence and graphene from the molecular level to provide assis-

*Project supported by the National Natural Science Foundation of China for Outstanding Young Scholars (Grant No. 11722548), the China Postdoctoral Science Foundation (Grant No. 2019M651462), the National Natural Science Foundation of China (Grant No. U1932123), the Innovative Research Team of High-Level Local Universities in Shanghai, the Open Project of State Key Laboratory of Advanced Special Steel, Shanghai Key Laboratory of Advanced Ferrometallurgy and the Science and Technology Commission of Shanghai Municipality (Gant No. 19DZ2270200), the Deepcomp7000 and ScGrid of Supercomputing Center, Computer Network Information Center of the Chinese Academy of Sciences, the Special Program for Applied Research on Super Computation of the NSFC–Guangdong Joint Fund (second phase), the Shanghai Supercomputer Center of China, the High Performance Computing Platform of Shanghai University.

†Corresponding author. E-mail: gsshi@shu.edu.cn

© 2021 Chinese Physical Society and IOP Publishing Ltd

tance for the design and application of graphene-based DNA biosensor. Methyl phosphate[33] can be regarded as a simple analog of phosphate moieties in DNA/RNA to research the interaction between multivalent anions and the electron-rich graphene.

In this work, using DFT calculations, we take methyl phosphate as an example to investigate the interactions between multivalent anions (PO_4^{3-}, $CH_3PO_4^{2-}$, $(CH_3)_2PO_4^-$) and the graphene flake ($C_{84}H_{24}$). We found that as the valence of anion increased from negative monovalence to negative trivalence, the interaction significantly increased. The adsorption energy of $(CH_3)_2PO_4^-$ on the electron-rich graphene flake ($C_{84}H_{24}$) is −8.3 kcal/mol. The adsorption energy between negative divalent anion ($CH_3PO_4^{2-}$) and the graphene flake ($C_{84}H_{24}$) is −48.0 kcal/mol, which is about six times of that between negative monovalent anion (($(CH_3)_2PO_4^-$) and the graphene flake ($C_{84}H_{24}$), and is even larger than that CO_3^{2-} adsorption on electron-deficient aromatic ring C_6F_6 (−28.4 kcal/mol).[1] The adsorption energy between negative trivalent anion (PO_4^{3-}) and graphene flake ($C_{84}H_{24}$) is −159.2 kcal/mol, which is about 20 times of that between negative monovalent anion (($(CH_3)_2PO_4^-$) and the graphene flake ($C_{84}H_{24}$). The energy decomposition analysis indicated that the super-strong adsorption energy is mainly attributed to the orbital interactions between multivalent anions and graphene. Meanwhile, the adsorption of anions decreased the HOMO–LUMO (highest occupied molecular orbital–lowest unoccupied molecular orbital) gap of the systems, which benefits the enhancement of electrical conductivity.

2. Methods

We performed DFT calculations using B3LYP method to describe the intermolecular interactions with the Gaussian-16 package.[34] The electron wave functions in the Gaussian function basis are used. For geometry optimization, the double-ζ basis is used. At the same time, we introduce a diffuse function into the basis set and add a d-polarization function to carbon atoms, phosphorus atoms, and oxygen atoms, respectively, as well as one p-polarization function to the hydrogen atoms [marked with 6-31+G(d,p)]. The geometry optimizations were performed via the Berny algorithm with the convergence criteria of a maximum step size of 0.0018 a.u. and a root-mean-square (RMS) force of 0.0003 a.u. We also calculated the single-point energy with dispersion-corrected DFT functional ωB97X-D to show the effect of dispersion interaction at ωB97X-D/6-31+G(d,p) level. We have taken a small system of PO_4^{3-} interaction with benzene as an example and performed the calculations with different methods and basis sets (see details in Supplementary material PS1), the results showed that calculation at the ωB97X-D//B3LYP/6-31+G(d,p) level is suitable for the research about the interaction between anions and graphene. We decomposed the total interaction energy into electrostatic interaction, Pauli repulsion and orbital interactions via an energy decomposition analysis (EDA) at the B3LYP method (the basis set of C, H, P, and O are TZP, TZP, ET-QZ3P-1DIFFUSE, and ET-QZ3P-1DIFFUSE, respectively) in the framework of DFT in the ADF program.[35]

3. Results and discussion

We first performed the geometry optimizations of different anions adsorption on hydrogenated-graphene flake ($C_{84}H_{24}$). Figure 1 shows the most stable geometry-optimized structures of different anions (PO_4^{3-}, $CH_3PO_4^{2-}$, $(CH_3)_2PO_4^-$) adsorption on the graphene surface. The negative trivalent PO_4^{3-} was adsorbed to the graphene surface with two oxygen atoms forming covalent bonds with the meta-carbon atoms of hexagonal ring. The average nearest oxygen–carbon distance was 1.513 Å. Two meta-carbon atoms on the graphene flake surface close to PO_4^{3-} were pulled up, resulting to the deformation of the graphene flake. We noted that PO_4^{3-} is unstable in the gas phase,[36,37] it can exist in the solution with high pH,[38,39] in this situation PO_4^{3-} is hydrated by water molecules, thus we further calculated the hydrated PO_4^{3-} adsorption on the graphene flake, (see details in Supplementary material PS2). Figure S2 shows that as the number of water molecules increased, the adsorption energy decreased. When PO_4^{3-} is hydrated by three water molecules, the adsorption energy is −77.3 kcal/mol, which is about 130 k_BT ($\sim$ 16 times hydrogen bonds between water molecules) at the room temperature, thus can be stable adsorbed on the graphene flake.

The negative bivalent $CH_3PO_4^{2-}$ was adsorbed on the graphene surface with two oxygen atoms locating above the C–C bond on the para position of hexagonal ring, the average nearest oxygen–carbon distance was 2.778 Å. The negative monovalent $(CH_3)_2PO_4^-$ was adsorbed on the graphene surface with two dangling oxygen atoms locating above the C–C bond on the para position of hexagonal ring and other two oxygen atoms saturated by methyl locating above the para-carbon atoms of hexagonal ring. The average nearest oxygen–carbon distance was 3.080 Å. As the valence of anion increased from negative monovalence to negative trivalence, the average nearest oxygen–carbon distance gradually decreased.

We calculated the adsorption energy with the formula

$$E_{\text{ads}} = E_{\text{anion@G}} - E_{\text{G}} - E_{\text{anion}}, \tag{1}$$

where $E_{\text{anion@G}}$, E_{G}, and E_{anion} are the total energy of the anion adsorption on a graphene flake, the isolated anion, and a graphene flake, respectively. For different anions, the adsorption energies, average nearest oxygen–carbon distances, and transfer Mullikan charges are shown in Table 1.

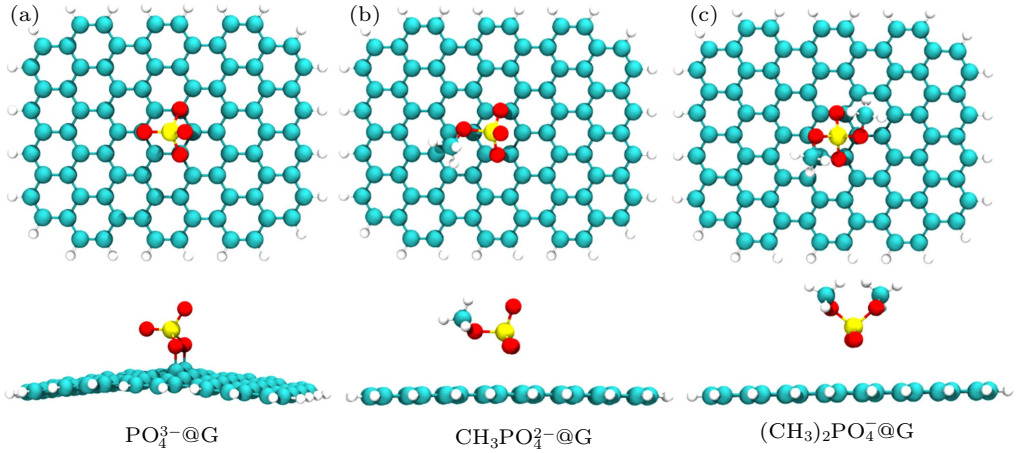


Fig. 1. Top and side views of the most stable geometry-optimized structures of different anions PO_4^{3-} (a), $CH_3PO_4^{2-}$ (b), and $(CH_3)_2PO_4^-$ (c) adsorption on the graphene flake (G), respectively. Atoms are colored as follows: C, cyan; O, red; P, yellow; H, white.

Table 1. Adsorption energies (E_{ads}), average nearest oxygen–carbon distance ($R_{oxygen-C}$), and transfer Mullikan charges for different anions adsorption on the graphene flake at B3LYP/6-31+G(d,p) level. "–" in transfer Mullikan charge represents that the anions lose electrons. Adsorption energies (E'_{ads}) for different anions adsorption on the graphene flake at ωB97X-D/6-31+G(d,p)//B3LYP/6-31G+(d,p) level.

Anions–graphene clusters	E_{ads} (kcal/mol)	E'_{ads} (kcal/mol)	$R_{oxygen-C}$ (Å)	Transfer Mullikan charge
PO_4^{3-}@G	−159.2	−173.0	1.513	−2.675
$CH_3PO_4^{2-}$@G	−48.0	−45.9	2.778	−0.778
$(CH_3)_2PO_4^-$@G	−8.3	−15.7	3.080	−0.009

From Table 1, the adsorption energy of PO_4^{3-} is −159.2 kcal/mol at B3LYP/6-31+G(d,p) level, which is about 20 times that of $(CH_3)_2PO_4^-$ (−8.3 kcal/mol) and is about three times that of $CH_3PO_4^{2-}$ (−48.0 kcal/mol) at B3LYP/6-31+G(d,p) level. This indicates that as the valence of anion increased from negative monovalence to negative trivalence, the interaction remarkably increased. We also calculated the adsorption energy at ωB97X-D/6-31+G(d,p)//B3LYP/6-31G+(d,p) level to show the effect of dispersion interaction. As shown in Table 1, As the valence of anion increased from negative monovalence to negative trivalence, the adsorption energy significantly increases, which is in agreement with the results using B3LYP/6-31+G(d,p). The dispersion interaction has some effect on the specific value of adsorption energy. The adsorption energy of PO_4^{3-} was −173.0 kcal/mol and increased to 13.8 kcal/mol compared to the adsorption energy (−159.2 kcal/mol) using B3LYP/6-31+G(d,p). The adsorption energy of $CH_3PO_4^{2-}$ was −45.9 kcal/mol and decreased to 2.1 kcal/mol compared to the adsorption energy (−48.0 kcal/mol) using B3LYP/6-31+G(d,p). The adsorption energy of $(CH_3)_2PO_4^-$@G was −15.7 kcal/mol and increased to 7.4 kcal/mol compared to the adsorption energy (−8.3 kcal/mol) using B3LYP/6-31+G(d,p). We have also researched how the size of graphene flake affects their interaction, as the size of graphene flake increased, the adsorption energy between anions and graphene increased. As the valence of anion increased from negative monovalence to negative trivalence, the adsorption energy increased on the same size of graphene (see details in Supplementary material PS3).

To understand the super-strong interactions between multivalent anions and the graphene flake, we performed the Mulliken charges analysis. Figure 2 shows the Mulliken charges distribution of different anions adsorption on the graphene flake (see details in Supplementary material PS4). The residual Mulliken charge of PO_4^{3-} is −0.325 e after PO_4^{3-} adsorption on the graphene flake ($C_{84}H_{24}$), which demonstrates electron is easier to transfer from the anion to the graphene flake ($C_{84}H_{24}$) and the graphene flake ($C_{84}H_{24}$) exhibits strong electron-withdrawing ability and accept partial electron during the anion adsorption. The PO_4^{3-} loses partial electrons (2.685 e) and transfers these electrons to the graphene flake. The transfer Mulliken charge is calculated by the difference of initial Mulliken charge of the isolated anions and the residual Mulliken charge after anions adsorption on the graphene flake. The residual Mulliken charge of $CH_3PO_4^{2-}$ is −1.222 e after $CH_3PO_4^{2-}$adsorption on the graphene flake ($C_{84}H_{24}$) and the residual Mulliken charge of $(CH_3)_2PO_4^-$ is −0.991 e after $(CH_3)_2PO_4^-$ adsorption on the graphene flake ($C_{84}H_{24}$). From Table 1, the amount of transfer Mulliken charges between different valence anions and the graphene flakce ($C_{84}H_{24}$) increased as the valence of anion increased from negative monovalence to negative trivalence, which indicated the more charge transfer, the stronger interaction between anions and the graphene flake. We also performed the Hirshelf charge analysis and listed the transfer Hirshfeld charge in Table S2 in Supplementary material. The amount of transfer Hirshelf charges between different valence anions and the graphene flakce ($C_{84}H_{24}$) increased as the valence of anion increased from negative monovalence to negative trivalence, which is in agreement with that of transfer Mulliken charge. We also note

that the adsorption of anions decreased the HOMO–LUMO gap of the systems, which benefits the enhancement of electrical conductivity (see details in Supplementary material PS6).

We also performed the molecular orbitals analysis. We checked the occupied molecular orbitals from highest occupied molecular orbital (HOMO) to HOMO-6. Figure 3 shows the representatives of molecular orbitals of the interactions between different anions and the graphene flake. Four occupied molecular orbitals (HOMO-2, HOMO-3, HOMO-4, and HOMO-6) of PO_4^{3-}@G complex, three occupied molecular orbitals (HOMO-2, HOMO-3, and HOMO-6) of $CH_3PO_4^{2-}$@G complex and two occupied molecular orbitals (HOMO-4 and HOMO-5) of $(CH_3)_2PO_4^-$ complex were plotted, which indicated the electron delocalized distribution of the graphene was disturbed when anions were adsorbed on the graphene surface and the clearly coupling between the delocalized π orbitals of graphene and the molecular orbital of anions. The other molecular orbitals of the interactions between different anions and the graphene flake ($C_{84}H_{24}$) can be seen in Supplementary material PS5. The nature of bonding can be characterized by the values of electron density (ρ) and the sign of the Laplacian of electron density ($\nabla^2\rho$). Higher ρ values along with negative $\nabla^2\rho$ values are indicative of interactions involving covalent interaction. Lower ρ values along with positive $\nabla^2\rho$ values are indicative of interactions involving non-covalent interaction.[40] We further performed the atoms in molecules (AIM) analysis using Multiwfn[41] to distinguish whether the interaction between anions with different valence states, and graphene is covalent interaction or non-covalent interaction and listed the data in Table 2. The AIM analysis indicated that PO_4^{3-} surely formed covalent bond between oxygen atom and the nearest carbon atoms of graphene, $CH_3PO_4^{2-}$ and $(CH_3)_2PO_4^-$ formed non-covalent bond with graphene, and the bond strength between $CH_3PO_4^{2-}$ and graphene is larger than that between $(CH_3)_2PO_4^-$ and graphene.

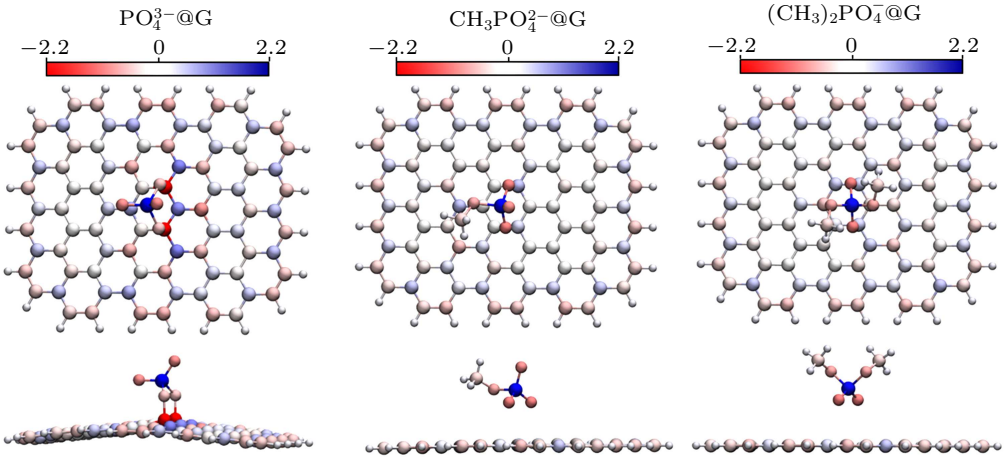


Fig. 2. Mulliken charges distribution of different anions adsorption on the graphene flake.

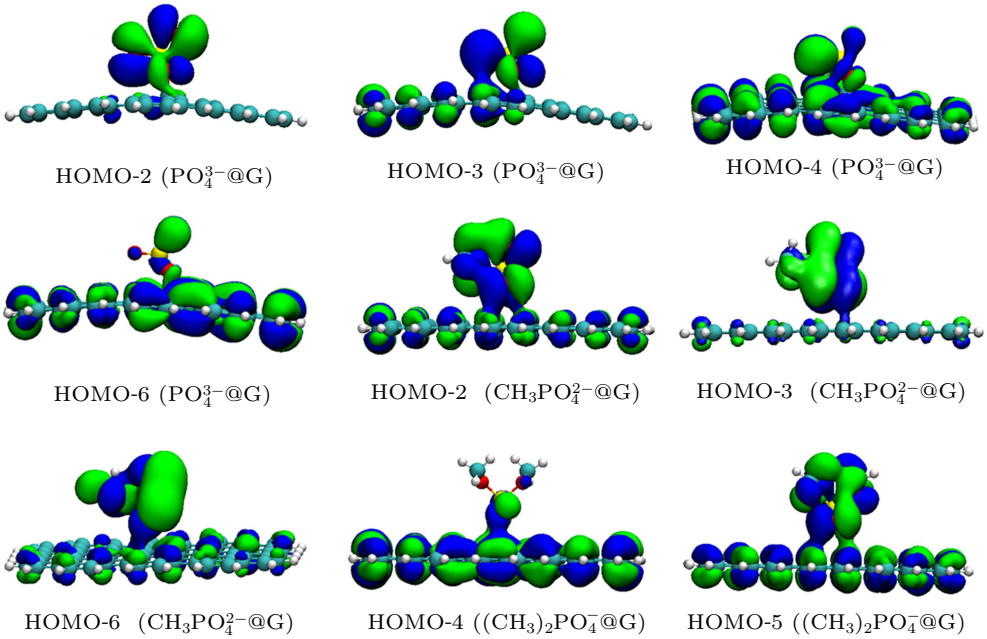


Fig. 3. The representatives of occupied molecular orbital for PO_4^{3-}@G, $CH_3PO_4^{2-}$@G, and $(CH_3)_2PO_4^-$@G, respectively. The atoms are colored as follows: C: cyan; H: white; O: red; P: yellow. The molecular orbital is plotted with iso-values of ±0.01 a.u., where blue and green areas denote opposite signs (±) of the orbital phase.

Table 2. Bond critical point properties [electron density (ρ); Laplacian of electron density ($\nabla^2\rho$); potential energy density (V_b); Lagrangian kinetic energy (G_b); energy density H_b] of oxygen and carbon bonds in the studied complexes at the B3LYP/6-31+G(d,p) level.

Anions–graphene clusters	ρ	$\nabla^2\rho$	V_b	G_b	H_b	$\lvert V_b\rvert/G_b$
PO_4^{3-}@G	0.211	−0.317	0.323	0.122	0.201	2.648
$CH_3PO_4^{2-}$@G	0.015	0.049	−0.01	0.011	0.001	0.909
$(CH_3)_2PO_4^-$@G	0.009	0.028	−0.05	0.006	0.001	0.833

Moreover, to illustrate the underlying physics of the interactions, we performed the energy decomposition analysis (EDA) using ADF program.[35] As shown in Table 3, the total interaction energies between anions (PO_4^{3-}, $CH_3PO_4^{2-}$, $(CH_3)_2PO_4^-$) and the graphene flake ($C_{84}H_{24}$) were decomposed into Pauli repulsion, orbital interaction and electrostatic interaction. The EDA results showed that the attractive energy is mainly attributed to the orbital interaction, the repulsive energy is mainly attributed to Pauli repulsion and electrostatic interaction for the $(CH_3)_2PO_4^-$ adsorption on the graphene flkae ($C_{84}H_{24}$). The attractive energy is mainly attributed to the orbital interaction and electrostatic interaction, the repulsive energy is mainly attributed to Pauli repulsion for the multivalent anions (PO_4^{3-}, $CH_3PO_4^{2-}$) adsorption on the graphene flkae ($C_{84}H_{24}$).

We also investigated the hydrogenated phosphate anions (HPO_4^{2-}, $H_2PO_4^-$) adsorption on the graphene flake ($C_{84}H_{24}$), the adsorption energy of $H_2PO_4^-$ is −5.3 kcal/mol, which is smaller than that of $(CH_3)_2PO_4^-$ (−8.3 kcal/mol). The adsorption energy of HPO_4^{2-} is −49.7 kcal/mol, which is slighter larger than that of $CH_3PO_4^{2-}$ (−48.0 kcal/mol). The adsorption energy of hydrogenated phosphate anions also increased as the valence of anions increase from negative monovalence to negative trivalence, which is in agreement with that of methyl phosphate anions. These results indicated the functional groups type to saturate the dangling oxygen atom of phosphate anion has little effect on the interaction between different valence phosphate anions and the graphene flake. The detailed discussions about molecular orbital analysis and Mulliken charge distribution of hydrogenated phosphate anions (HPO_4^{2-}, $H_2PO_4^-$) adsorption on graphene flake ($C_{84}H_{24}$) can be seen in Supplementary material PS7.

Table 3. Electrostatic interaction, Pauli repulsion, and orbital interaction between anions with different valance and graphene calculated at the B3LYP method.

Anions–graphene clusters	Pauli repulsion (kcal/mol)	Orbital interaction (kcal/mol)	Electrostatic interaction (kcal/mol)
PO_4^{3-}@G	771.79	−601.21	−375.82
$CH_3PO_4^{2-}$@G	34.98	−77.02	−6.64
$(CH_3)_2PO_4^-$@G	9.13	−16.4	2.67

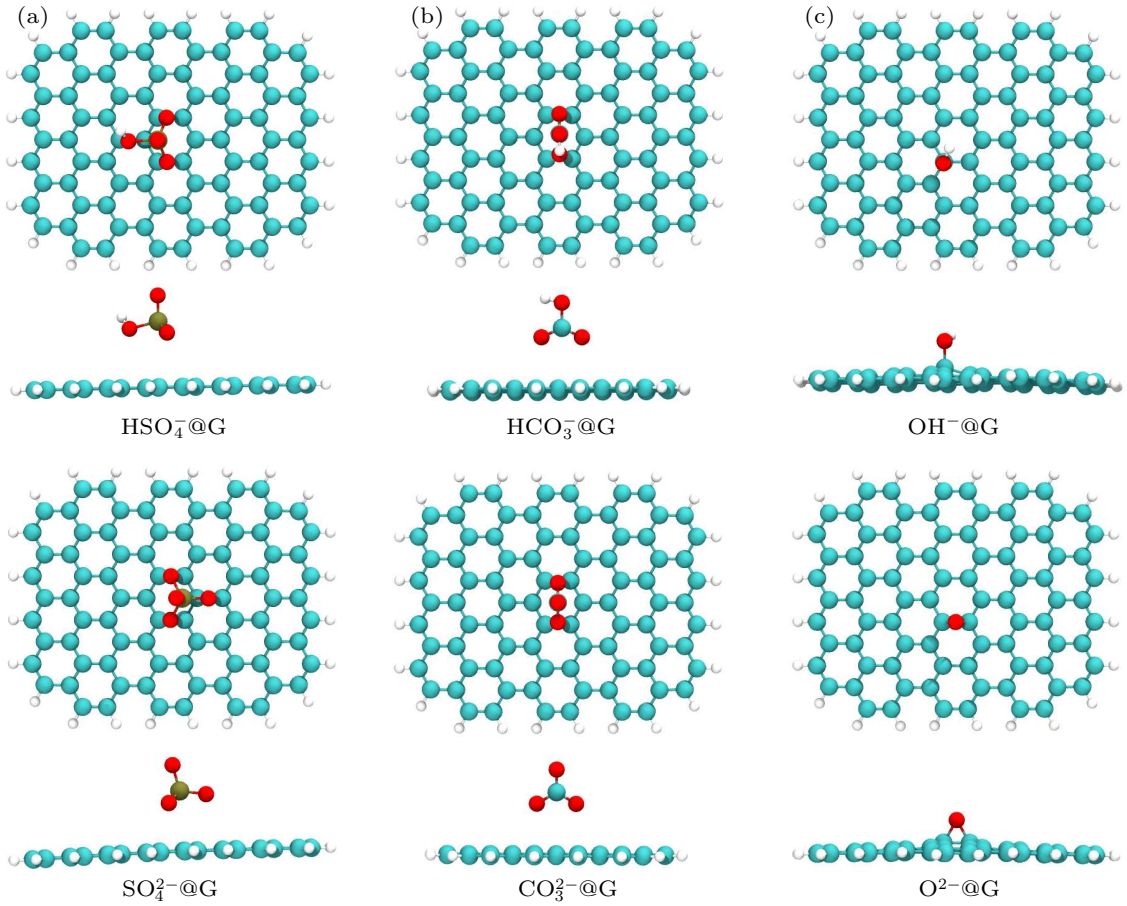


Fig. 4. Top and side views of the most stable geometry-optimized structures of HSO_4^-/SO_4^{2-}, HCO_3^-/CO_3^{2-}, and OH^-/O^{2-} adsorption on graphene flake, respectively. Atoms are colored as follows: C, cyan; O, red; S, brown; H, white.

We also calculated other anions of various charges (HSO_4^-/SO_4^{2-}, HCO_3^-/CO_3^{2-}, and OH^-/O^{2-}) interaction with the graphene flake. Figure 4 showed the optimized most stable structure of HSO_4^-/SO_4^{2-}, HCO_3^-/CO_3^{2-}, and OH^-/O^{2-} adsorption on graphene flake, respectively. We have listed the adsorption energy of all the anions calculated in Fig. 5. The results showed that the adsorption energy of other anions of various charges is also larger than that of the corresponding monovalent anion, which are in agreement with the results as the valence of anion increased, the adsorption energy increased. The AIM analysis (Table S8) indicates that OH^-/O^{2-} also formed covalent bonds with graphene flake, the average nearest oxygen–carbon distance of O^{2-} (1.475 Å) adsorption on graphene flake is smaller than that of PO_4^{3-} (1.513 Å) adsorption on graphene flake, and the adsorption energy of O^{2-} is larger than that of PO_4^{3-}.

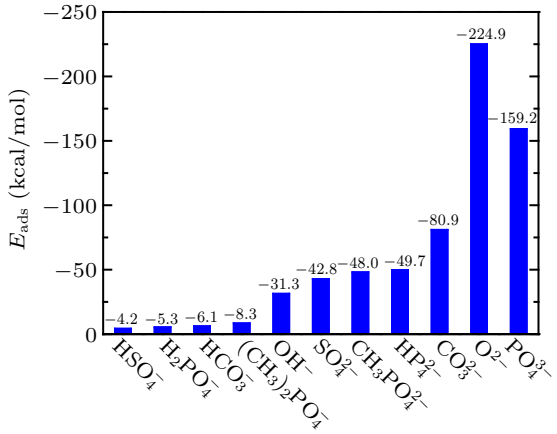


Fig. 5. Adsorption energy of different anions adsorptions on the graphene flake at the B3LYP/6-31G+(d,p) level.

4. Conclusion

In conclusion, based on DFT calculations, we investigated the interactions between different valence anions (PO_4^{3-}, $CH_3PO_4^{2-}$, $(CH_3)_2PO_4^-$) and the graphene flkae ($C_{84}H_{24}$), and found that the valence of anion increased from negative monovalence to negative trivalence, the interaction remarkably increased, which was mainly due to the orbital interactions between the multivalent anions and graphene flkae ($C_{84}H_{24}$). Meanwhile, the adsorption of anions decreased the HOMO–LUMO energy gap of the systems, which is beneficial to the enhancement of electrical conductivity. We also researched hydrogenated phosphate anions (HPO_4^{2-}, $H_2PO_4^-$) adsorption on graphene flake ($C_{84}H_{24}$), and found that adsorption energy of hydrogenated phosphate anions (PO_4^{3-}, HPO_4^{2-}, $H_2PO_4^-$) also increased as the valence of anions increased from negative monovalence to negative trivalence, and the functional groups type to saturate the dangling oxygen atom of phosphate anion has little effect on the interaction between different valence phosphate anions and the graphene flake. The adsorption energy of other bivalent anion (SO_4^{2-}, CO_3^{2-}, and O^{2-}) is also larger than that of the corresponding monovalent anion (HSO_4^-, HCO_3^-, and OH^-).

Comparing to the monovalent halide anions adsorption on the graphene flake (the $F^-/Cl^-/Br^-$ adsorption energies are −16.3 kcal/mol, −7.7 kcal/mol, and −6.0 kcal/mol, respectively), the adsorption of multivalent anions on graphene flake ($PO_4^{3-}/CH_3PO_4^{2-}$ adsorption energies are −152.9 kcal/mol, −48.0 kcal/mol, respectively) should be considered as 'super strong', even larger than the cation–π interaction between common alkali and graphene (the Na^+/K^+ adsorption energies are −39.6 kcal/mol, −28.7 kcal/mol).[42,43] Thus, these remarkably strong interactions between high valence anions and graphene cannot be ignored in the related research fields.

This work provides new insights for understanding the interactions between multivalent anions and π–electron-rich carbon-based nanomaterials and is helpful for design and application of graphene-based DNA biosensor.

References

[1] Quiñonero D, Garau C, Rotger C, Frontera A, Ballester P, Costa A and Deyà P M 2002 *Angew. Chem. Int. Ed.* **41** 3389
[2] Alkorta I, Rozas I and Elguero J 2002 *J. Am. Chem. Soc.* **124** 8593
[3] Mascal M, Armstrong A and Bartberger M D 2002 *J. Am. Chem. Soc.* **124** 6274
[4] Kim D, Tarakeshwar P and Kim K S 2004 *J. Phys. Chem. A* **108** 1250
[5] Schottel B L, Chifotides H T and Dunbar K R 2008 *Chem. Soc. Rev.* **37** 68
[6] Caltagirone C and Gale P A 2009 *Chem. Soc. Rev.* **38** 520
[7] Estarellas C, Frontera A, Quiñonero D and Deyà P M 2011 *Angew. Chem. Int. Ed.* **50** 415
[8] Frontera A, Gamez P, Mascal M, Mooibroek T J and Reedijk J 2011 *Angew. Chem. Int. Ed.* **50** 9564
[9] Wang D X and Wang M X 2013 *J. Am. Chem. Soc.* **135** 892
[10] Chifotides H T and Dunbar K R 2013 *Acc. Chem. Res.* **46** 894
[11] Lucas X, Bauzá A, Frontera A and Quiñonero D 2016 *Chem. Sci.* **7** 1038
[12] Xi J and Xu X 2016 *Phys. Chem. Chem. Phys.* **18** 6913
[13] Anstöter C S, Rogers J P and Verlet J R R 2019 *J. Am. Chem. Soc.* **141** 6132
[14] Zhang J, Xiang L, Yan B and Zeng H 2020 *J. Am. Chem. Soc.* **142** 1710
[15] Garau C, Frontera A, Quiñonero D, Russo N and Deyà P M 2011 *J. Chem. Theory Comput.* **7** 3012
[16] Lucas X, Quiñonero D, Frontera A and Deyà P M 2009 *J. Phys. Chem. A* **113** 10367
[17] Shi G, Yang J, Ding Y and Fang H 2014 *ChemPhysChem* **15** 2588
[18] Shi G, Ding Y and Fang H 2012 *J. Comput. Chem.* **33** 1328
[19] Lu C H, Yang H H, Zhu C L, Chen X and Chen G N 2009 *Angew. Chem. Int. Ed.* **48** 4785
[20] Yang W, Ratinac K R, Ringer S P, Thordarson P, Gooding J J and Braet F 2010 *Angew. Chem. Int. Ed.* **49** 2114
[21] Sassolas A, Leca-Bouvier B D and Blum L J 2008 *Chem. Rev.* **108** 109
[22] Min S K, Kim W Y, Cho Y and Kim K S 2011 *Nat. Nanotechnol.* **6** 162
[23] Tang L, Wang Y and Li J 2015 *Chem. Soc. Rev.* **44** 6954
[24] Xu Z, Lei X, Tu Y, Tan Z J, Song B and Fang H 2017 *Chem. - Eur. J.* **23** 13100
[25] Lei X, Ma H and Fang H 2020 *Nanoscale* **12** 6699
[26] Ma H, Xu Z, Fang H and Lei X 2020 *Phys. Chem. Chem. Phys.* **22** 11740
[27] Antony J and Grimme S 2008 *Phys. Chem. Chem. Phys.* **10** 2722
[28] Sowerby S J, Cohn C A, Heckl W M and Holm N G 2001 *Proc. Natl. Acad. Sci.* **98** 820
[29] Gowtham S, Scheicher R H, Ahuja R, Pandey R and Karna S P 2007 *Phys. Rev. B* **76** 033401
[30] Varghese N, Mogera U, Govindaraj A, Das A, Maiti P K, Sood A K and Rao C N R 2009 *ChemPhysChem* **10** 206

[31] Westheimer F H 1987 *Science* **235** 1173
[32] Watson J D and Crick F H C 1953 *Nature* **171** 737
[33] Villa F, MacKerell A D, Roux B and Simonson T 2018 *J. Phys. Chem. A* **122** 6147
[34] Frisch M J, Trucks G W, Schlegel H B, *et al.* 2016 *Gaussian* 16 *Rev. C*.01 (Wallingford, CT)
[35] te Velde G, Bickelhaupt F M, Baerends E J, Fonseca Guerra C, van Gisbergen S J A, Snijders J G and Ziegler T 2001 *J. Comput. Chem.* **22** 931
[36] Wang X B, Yang X, Nicholas J B and Wang L S 2001 *Science* **294** 1322
[37] Boldyrev A I and Simons J 1994 *J. Phys. Chem.* **98** 2298
[38] Pluhařová E, Ončák M, Seidel R, Schroeder C, Schroeder W, Winter B, Bradforth S E, Jungwirth P and Slavíček P 2012 *J. Phys. Chem. B* **116** 13254
[39] Sakulpaisan S, Vongsetskul T, Reamouppaturm S, Luangkachao J, Tantirungrotechai J and Tangboriboonrat P 2016 *J. Environ. Manage.* **167** 99
[40] Mahadevi A S and Sastry G N 2013 *Chem. Rev.* **113** 2100
[41] Lu T and Chen F 2012 *J. Comput. Chem.* **33** 580
[42] Shi G, Liu J, Wang C, Song B, Tu Y, Hu J and Fang H 2013 *Sci. Rep.* **3** 3436
[43] Shi G S, Wang Z G, Zhao J J, Hu J and Fang H P 2011 *Chin. Phys. B* **20** 068101